Stem Cell Reports
Article
ISSCR
OPEN ACCESS

Neurovascular Recovery via Cotransplanted Neural and Vascular Progenitors Leads to Improved Functional Restoration after Ischemic Stroke in Rats

Jia Li,[1,2,5] Yaohui Tang,[2,5] Yongting Wang,[2] Rongbiao Tang,[3] Weifang Jiang,[4] Guo-Yuan Yang,[2,*] and Wei-Qiang Gao[1,2,*]

[1]State Key Laboratory of Oncogenes and Related Genes, Renji-Med X Clinical Stem Cell Research Center, Ren Ji Hospital, School of Medicine, Shanghai Jiao Tong University, Shanghai 200127, China
[2]School of Biomedical Engineering and Med-X Research Institute, Shanghai Jiao Tong University, Shanghai 200030, China
[3]Department of Radiology, Ruijin Hospital, School of Medicine, Shanghai Jiao Tong University, Shanghai 200030, China
[4]Institute of Neuroscience, Shanghai Institutes for Biological Sciences, Chinese Academy of Sciences, Shanghai 200030, China
[5]Co-first author
*Correspondence: gyyang0626@gmail.com (G.-Y.Y.), gao.weiqiang@sjtu.edu.cn (W.-Q.G.)
http://dx.doi.org/10.1016/j.stemcr.2014.05.012

SUMMARY

The concept of the "neurovascular unit," emphasizing the interactions between neural and vascular components in the brain, raised the notion that neural progenitor cell (NPC) transplantation therapy aimed at neural repair may be insufficient for the treatment of ischemic stroke. Here, we demonstrate that enhanced neurovascular recovery via cotransplantation of NPCs and embryonic stem cell-derived vascular progenitor cells (VPCs) in a rat stroke model is correlated with improved functional recovery after stroke. We found that cotransplantation promoted the survival, migration, differentiation, and maturation of neuronal and vascular cells derived from the cotransplanted progenitors. Furthermore, it triggered an increased generation of VEGF-, BDNF-, and IGF1-expressing neural cells derived from the grafted NPCs. Consistently, compared with transplantation of NPCs alone, cotransplantation more effectively improved the neurobehavioral deficits and attenuated the infarct volume. Thus, cotransplantation of NPCs and VPCs represents a more effective therapeutic strategy for the treatment of stroke than transplantation of NPCs alone.

INTRODUCTION

Stroke is the third leading cause of death and disability in developed countries (van der Worp and van Gijn, 2007). Although immediate intervention with tissue plasminogen activator (TPA) can provide some benefits during the acute phase of stroke, no other clinically effective treatments are currently available for this disease (van der Worp and van Gijn, 2007). Stem cell transplantation represents a potential therapeutic strategy for stroke (Liu et al., 2014). Previous studies on stem cell transplantation emphasized the replacement of either neural or vascular components in the brain; however, the poor survival and differentiation of both the transplanted cells and their progenies in the hostile environment of the infarcted cortex hamper the efficacy of treatment (Martino and Pluchino, 2006; Kaneko et al., 2012).

The "neurovascular unit" of the brain provides a concept to consider improving the vasculature and other microenvironmental components to alleviate severe neural cell death that occurs after stroke, brain injury, and neurodegeneration, and comprises neurons, glia (astrocytes, microglia, and oligodendroglia), and vascular cells (endothelia, pericytes and vascular smooth muscle cells) (Zlokovic, 2010). The neurovascular signaling that can modulate various degrees of neuronal plasticity may be critically important for functional neurological recovery after CNS injury (Moskowitz et al., 2010). Consequently, it has been suggested that therapeutic approaches should target both neural and vascular cell types in order to protect their structural and functional integrity and their reciprocal interactions (Zlokovic, 2010; Moskowitz et al., 2010). In this regard, Nakagomi et al., (2009) reported that in a mouse stroke model, cotransplantation of endothelial cells (ECs) together with neural stem/progenitor cells enhanced the survival, proliferation, and differentiation of the neural stem/progenitor cells and partly improved cortical function (locomotion under the light condition). However, whether cotransplantation of neural progenitor cells (NPCs) with vascular progenitor cells (VPCs) that produce multiple vascular elements, including pericytes/smooth muscle cells (SMAs), would yield a more effective functional recovery after focal ischemic injury in the cortex compared with transplantation of NPCs alone has not been determined.

NPCs derived from embryonic day 14 (E14) mice have been shown to differentiate into both neuronal and glial cells (Reynolds and Weiss, 1996) in vitro. Mouse embryonic stem cell-derived VPCs (ESC-VPCs) can differentiate into not only ECs but also vascular mural cells (pericytes/SMAs) (Yamashita et al., 2000), an important cell type that is involved in construction of the blood-brain barrier (Dalkara et al., 2011). In this study, we cotransplanted fetal NPCs and ESC-VPCs in a rat model of transient middle cerebral artery occlusion (tMCAO), a clinically relevant

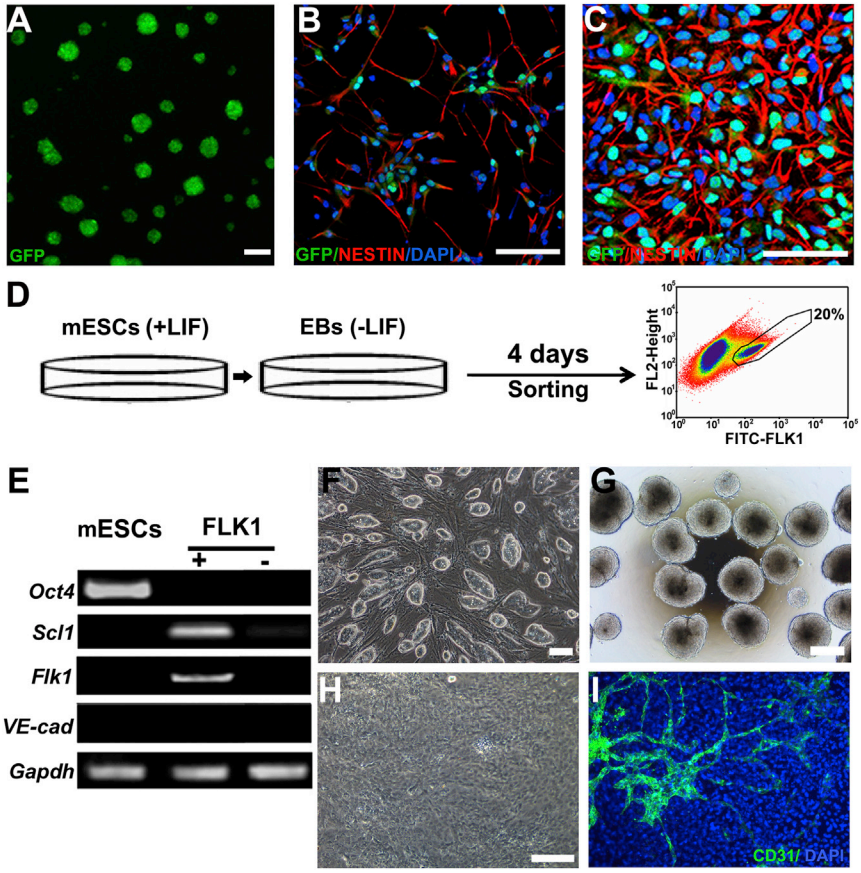

Figure 1. The Progenitor Cell Properties of NPCs and ESC-VPCs Were Maintained Prior to Transplantation

(A) Neurospheres derived from the telencephalon of E14 GFP transgenic mice.

(B and C) Dissociated cells in the neurospheres on a monolayer culture at 70% (B) or 95% (C) density were immunostained against the embryonic NPC marker NESTIN.

(D) Schematic diagram illustrating the procedure for deriving VPCs from ESCs.

(E) mRNA expression of specific marker genes in undifferentiated ESCs, FLK1$^+$, and FLK1$^-$ cell fractions in day 4 EBs. *VE-cad*, *VE-cadherin*. All RT-PCR experiments were performed in triplicate.

(F–I) ESCs maintained in an undifferentiated state (F) were forced to form EBs (G). After the EBs were cultured in suspension for 4 days, the FLK1$^+$ cell fraction was selected via FACS, seeded on mitomycin-C-irradiated fibroblasts, and exposed to VEGF. On day 11, the culture was immunostained against the EC-specific marker CD31. Bright-field (H) and fluorescence (I) images are shown. Scale bars, 100 μm.

model of focal cerebral ischemia. In addition, we used NPCs and VPCs of mouse origins in a rat stroke model to mimic interspecies cell transplantation. We found that cotransplantation of NPCs and VPCs facilitated the survival, differentiation, and/or maturation of neuronal and vascular cells derived from the cotransplanted progenitors. This beneficial effect of cotransplantation correlated with greater improvements in motor function of the affected limb and reduced infarct volume compared with NPC transplantation alone, providing evidence that fostering both neural and vascular recovery could be more effective than neural repair alone in promoting functional recovery from stroke-induced impairments.

RESULTS

Characterization of NPCs and VPCs before Transplantation

To generate NPCs that could be tracked after transplantation, we derived primary cells from the telencephalons of E14 transgenic mice, which express a GFP reporter under the control of a CMV promoter. A small proportion of the primary cells generated neurospheres by day 8 of the initial culture (Figure 1A). After collecting and expanding the cells in the neurospheres on fibronectin-coated plates for two passages, we characterized the cells via immunostaining against NESTIN, a marker of embryonic NPCs. As shown in Figures 1B and 1C, more than 97% of the GFP$^+$ cells expressed NESTIN, suggesting that the majority of the cells in the culture maintained a progenitor cell phenotype. The neurosphere cells that were expanded on the fibronectin-coated plates at passage 2 were then used for transplantation.

We employed an embryoid body (EB) approach to derive VPCs from mouse ESCs according to a previously described method (Li and Stuhlmann, 2012). After 4 days of culture as EBs, the fetal liver kinase 1 (FLK1)$^+$ cell fraction was selected from the EBs via fluorescence-activated cell sorting (FACS; Figure 1D), and an aliquot of the FLK1$^+$ cells was subjected to a panel of tests to evaluate the expression of various markers via RT-PCR (Figure 1E). These tests revealed that FLK1$^+$ cells lost expression of the undifferentiated ESC marker *Oct4*, expressed the hemangioblast markers *Scl/Tal1* and *Flk1*, and did not express the EC marker *VE-cadherin*. In contrast, the FLK1$^-$ cell fraction did not express any of the above markers, and the ESCs only expressed

Oct4 (Figure 1E). These results suggest that the FLK1$^+$ cells derived from the day 4 EBs were hemangioblasts (Lugus et al., 2009). To further elucidate whether the FLK1$^+$ hemangioblasts were able to develop the vasculature in vitro, the FLK1$^+$ or FLK1$^-$ cells were placed on mitomycin-C treated fibroblasts and exposed to VEGF (Figures 1F–1I). By day 11, the FLK1$^+$ cells developed highly branched vascular networks based on immunostaining against the EC marker CD31 (Figures 1H and 1I). In sharp contrast, the FLK1$^-$ cells did not form any vasculature under the same culture conditions at the same time point. The FLK1$^+$ hemangioblasts were thus defined as VPCs and used for transplantation.

Cotransplantation of NPCs and VPCs Promoted Graft Migration, Neural Graft Survival, Neuronal Differentiation, and/or Maturation

To address whether cotransplantation of NPCs and VPCs can promote graft migration, neural graft survival, neuronal differentiation, and/or maturation, we injected 1 million NPCs and 0.5 million VPCs (25 μl/mice) into the peri-infarct area of the injured rat brains (n = 6; Figure 2A). As controls, 1 million NPCs and 0.5 million gamma-irradiated embryonic fibroblast cells (irrFCs; inactive cells; 25 μl/mice) or 1 million NPCs alone (25 μl/mice) were injected into the same site of injured brains (n = 6 for each control group; Figure 2A). For lineage tracing, we used the fluorescent vital dye Hoechst 33342 (Ho), which binds DNA in live cells, to label VPCs and irrFCs prior to transplantation in all the experiments.

By day 14, transplanted cells migrated from the peri-infarct cortex into the infarct area in rats transplanted with NPCs alone (Figures 2A and 2B), rats cotransplanted with NPCs and irrFCs (Figure 2C), and rats cotransplanted with NPCs and VPCs (Figure 2D). To examine whether cotransplantation of NPCs and VPCs affects the migration of grafts, we measured the average vertical distance of the farthest migration. In the NPC and VPC cotransplantation group, cells migrated 4.0-fold farther than those in the NPC and irrFC cotransplantation group (2,833.0 ± 763.8 μm versus 700.0 ± 150.0 μm; $p < 0.01$) or 5.7-fold farther than those in the NPC-alone transplantation group (2,833.0 ± 763.8 μm versus 500.0 ± 132.3 μm; $p < 0.01$; Figure 2E).

To evaluate neural graft survival, we first performed a TUNEL assay to detect dead GFP$^+$ cells in the grafts. Less than 0.01% of the GFP$^+$ cells were TUNEL$^+$ in all of the groups examined on day 14 after transplantation (image not shown). However, we found that the number of grafted GFP$^+$ cells out of the total number of injected GFP$^+$ cells in rats cotransplanted with NPCs and VPCs was significantly higher than that in rats cotransplanted with NPCs and irrFCs (~2.5% versus ~1.1%; $p < 0.01$) or rats transplanted with NPCs alone (~2.5% versus ~1.0%; $p < 0.01$), suggesting that cotransplantation of NPCs and VPCs promotes neural graft survival (Figure 2F).

We then examined the differentiation of GFP$^+$ cells in the infarct area via immunostaining against a panel of neural markers, including NESTIN (a marker of neural stem cells), doublecortin (DCX, a marker of neuronal precursors), glial fibrillary acidic protein (GFAP, a marker of astroglial cells), βIII-TUBULIN (a marker of neurons), and TAU1 (a marker of mature neurons). We detected very few GFP$^+$/NESTIN$^+$ (<0.1%) or GFP$^+$/DCX$^+$ (<0.1%) cells in all of the three groups on day 14 (data not shown). Surprisingly, the majority of the GFP$^+$ cells expressed GFAP (Figures 2G–2K) and only a small portion of the GFP$^+$ cells expressed βIII-TUBULIN (Figures 2L and 2M) in rats transplanted with NPCs alone on day 14. A similar result was obtained for rats cotransplanted with NPCs and irrFCs (Figure S1 available online).

In the rats cotransplanted with NPCs and VPCs, a large number of GFP$^+$ and Ho$^+$ cells were detected in the infarct cortex (Figures 3A and 3B). When we labeled the vessels using dye-conjugated LECTIN and immunostaining against α-SMA, a marker of mural cells (Lopes et al., 2011), we detected many mural cell-covered Ho$^+$/LECTIN$^+$ microvessels, some of which were surrounded by GFP$^+$ cells in the infarct area (Figure 3C). Immunostaining against neuronal markers revealed a much higher percentage of GFP$^+$/βIII-TUBULIN$^+$ neurons (~70% versus ~23%; $p < 0.001$) and a lower percentage of GFP$^+$/GFAP$^+$ astroglial cells (~30% versus ~76%; $p < 0.001$) in the rats cotransplanted with NPCs and VPCs compared with those cotransplanted with NPCs and irrFCs or those transplanted with NPCs alone (Figure 3D). Additionally, whereas none of the GFP$^+$ cells expressed the mature neuronal marker TAU1 in the two control groups (image not shown), an average of 12.3% ± 1.6% of the GFP$^+$ cells expressed TAU1 in the group cotransplanted with NPCs and VPCs, suggesting much more mature neuronal differentiation (Figure 3D).

To further examine whether the engrafted neurons matured into specific neuronal subtypes, we stained the brain sections against γ-aminobutyric acid (GABA), a marker of GABAergic neurons, or glutamate vesicular transporter (VGLUT1), a marker of glutamatergic neurons. None of the GFP$^+$ cells stained positively for VGLUT1 in any of the three groups examined, and no GFP$^+$/GABA$^+$ cells were detected in the two control groups. However, some GFP$^+$ cells stained positively for GABA in the lower middle part of the cortex from the transplantation site (rectangular purple area in Figure 3A), which constituted 22.8% ± 3.6% of the engrafted GFP$^+$ cells in the rats cotransplanted with NPCs and VPCs (Figure 3E). Next, we performed double immunostaining against GABA and VGLUT1 to examine whether these cells received synaptic inputs. Double immunostaining revealed robust VGLUT1 staining on GFP$^+$/GABA$^+$ cell bodies,

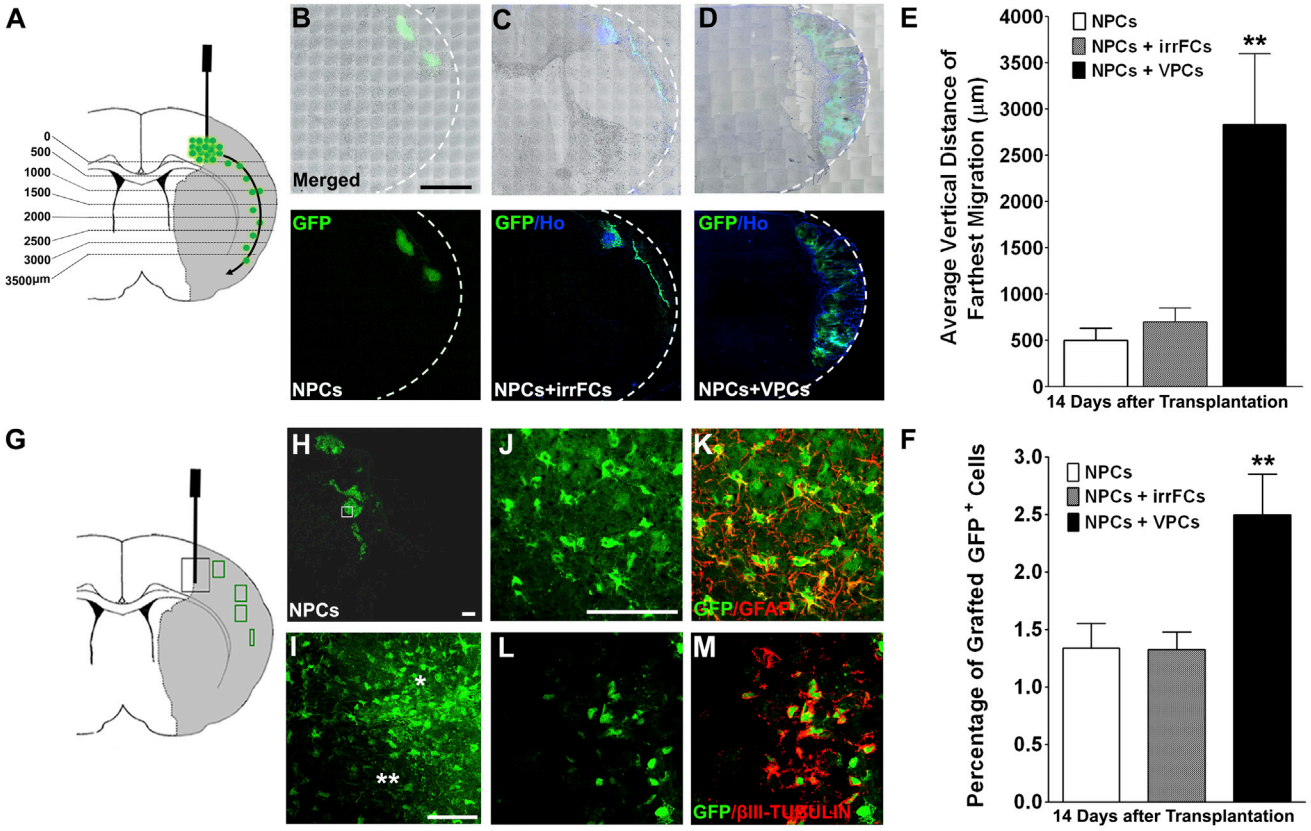

Figure 2. Cotransplantation of NPCs and VPCs Promoted Graft Migration and Neural Graft Survival

(A) Diagram illustrating the tour of cell migration in an injured brain. The infarct area is denoted in gray, the transplants are denoted in green aggregates, the arrow indicates the direction of migration, and the vertical distance away from the edge of transplants is labeled.

(B–D) Low-magnification images of transplants in rat brains in the group transplanted with NPCs alone (B), the group cotransplanted with NPCs and irrFCs (C), and the group cotransplanted with NPCs and VPCs (D) on day 14 after transplantation. Merged: merge of bright-field and fluorescence images.

(E) The average vertical distance of the farthest migration in rats cotransplanted with NPCs and VPCs was compared with that in rats cotransplanted with NPCs and irrFCs or rats transplanted with NPCs alone on day 14 after transplantation.

(F) The number of grafted GFP^+ cells out of the total number of injected GFP^+ cells in rats cotransplanted with NPCs and VPCs was compared with that in rats cotransplanted with NPCs and irrFCs or rats transplanted with NPCs alone on day 14 after transplantation.

(G) Diagram illustrating the injection (black box) and migration (green boxes) sites of neural transplants in a rat brain. The infarct area is denoted in gray.

(H) Low-magnification image of grafted GFP^+ cells in a rat brain transplanted with NPCs alone on day 14 after transplantation.

(I) Enlarged image of the boxed region in (H).

(J and K) The GFP^+ cells in the region marked by * in (I) were immunostained using antibodies against GFAP.

(L and M) The GFP^+ cells in the region marked by ** in (I) were immunostained using antibodies against βIII-TUBULIN.

The data are presented as means ± SD (**$p < 0.01$; one-way ANOVA and Tukey's post hoc). Scale bars, 2 mm in (B) and 100 μm otherwise. See also Figure S1.

suggesting that the grafted GABAergic neurons receive glutamatergic inputs (Figure 3E).

Cotransplantation of NPCs and VPCs Enhanced the Vascular Graft Survival, Differentiation, Formation, and Maturation of Microvessels

To determine whether cotransplantation of NPCs and VPCs can promote vascular graft survival and the differentiation, formation, and maturation of blood vessels, rats (n = 6) were transplanted with 0.5 million VPCs alone (25 μl/mice) and compared with rats (n = 6) cotransplanted with 1 million NPCs and 0.5 million VPCs (25 μl/mice). There were clusters of Ho^+ cells in both the rats transplanted with VPCs alone and the rats cotransplanted with NPCs and VPCs on day 14 (Figures 4A and 4B). TUNEL staining revealed that <0.01% of the Ho^+ cells

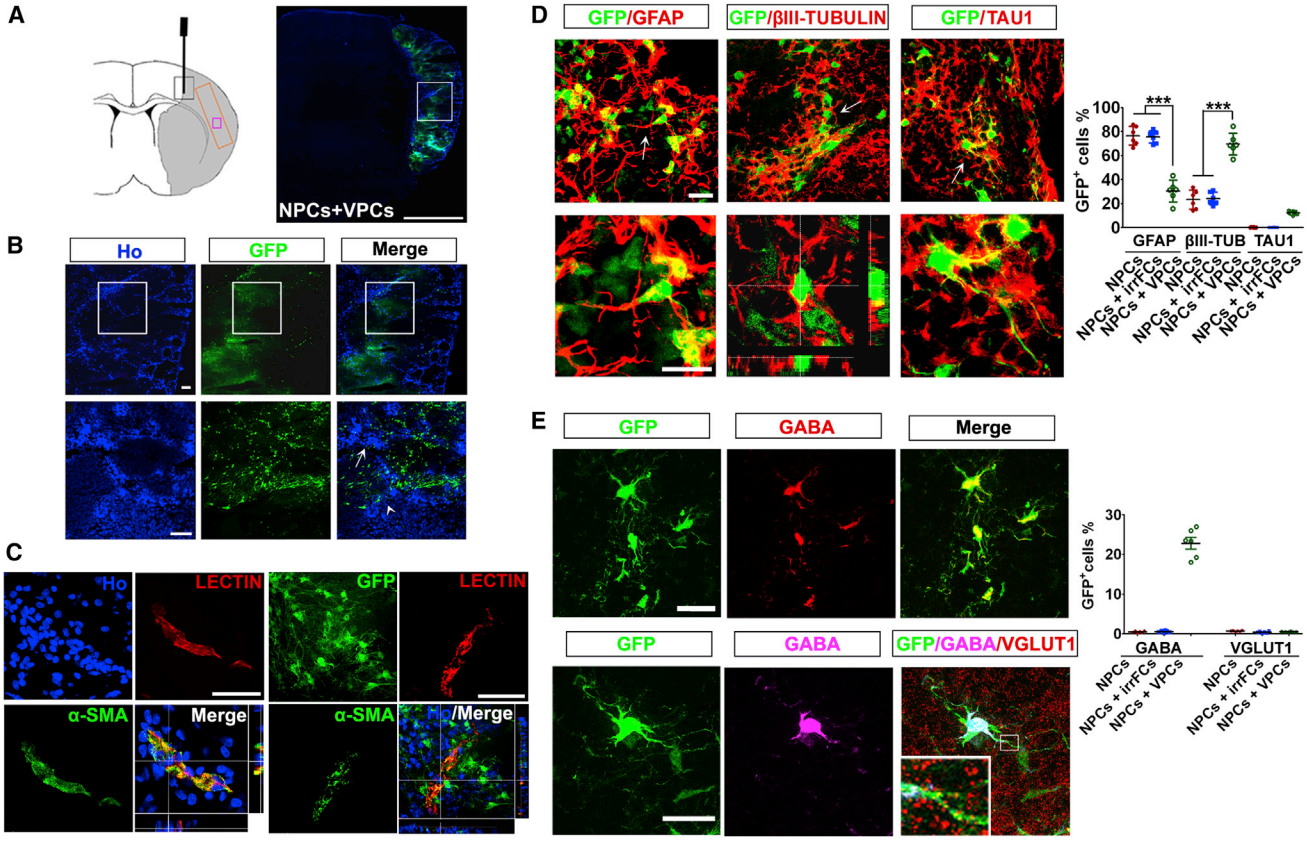

Figure 3. Cotransplantation of NPCs and VPCs Promoted the Differentiation and/or Maturation of Neuronal Cells Derived from Engrafted NPCs

(A) Left: diagram illustrating the injection (black box) and migration (orange box) sites of cotransplantation in a rat brain. The infarct area is denoted in gray. Right: low-magnification image of grafted GFP^+ and Ho^+ cells in a rat brain cotransplanted with NPCs and VPCs on day 14 after transplantation.

(B) Top: enlarged view of the white-boxed region in (A). Bottom: enlarged view of the white-boxed region in the upper panel.

(C) Rat brains were perfused with LECTIN before dissection. The sections were then immunostained using antibodies against α-SMA. Left: a representative image of a $LECTIN^+/\alpha\text{-}SMA^+$ microvessel generated by the Ho^+ cells in (B) (arrow). Right: a representative image of a $LECTIN^+/\alpha\text{-}SMA^+$ microvessel that is surrounded by GFP^+ cells and was generated by the Ho^+ cells in (B) (arrowhead). The x-z and y-z planes of the three-dimensional view of merge images are shown on the right and below, respectively.

(D) Left: the GFP^+ cells in (B) were immunostained using antibodies against GFAP, βIII-TUBULIN, or TAU1. Below is an enlarged view of the arrow-highlighted cells in the upper panel. Right: the numbers of $GFP^+/GFAP^+$, $GFP^+/\beta III\text{-}TUBULIN^+$, and $GFP^+/TAU1^+$ cells out of the total number of grafted GFP^+ cells in the infarct area in the group cotransplanted with NPCs and VPCs were compared with those in the group cotransplanted with NPCs and irrFCs or the group transplanted with NPCs alone. βIII-TUB, βIII-TUBULIN.

(E) Left: the GFP^+ cells in (B) were immunostained using antibodies against GABA or coimmunostained using antibodies against GABA and VGLUT1. Insets show the enlarged view of the boxed region. Right: the numbers of $GFP^+/GABA^+$ or $GFP^+/VGLUT1^+$ cells out of the total number of grafted GFP^+ cells in the infarct area in the group cotransplanted with NPCs and VPCs were compared with those in the group cotransplanted with NPCs and irrFCs or the group transplanted with NPCs alone.

The data are presented as means ± SD (***$p < 0.001$; Kruskal-Wallis test and Dunnett's post hoc). Scale bars, 2 mm in (A), 100 μm in (B) and (C), 20 μm in (D), and 40 μm in (E). See also Figure S1.

were $TUNEL^+$ in the grafts in both groups (image not shown). However, the number of grafted Ho^+ cells out of the total number of injected Ho^+ cells was ~2-fold higher in rats cotransplanted with NPCs and VPCs than in those transplanted with VPCs alone (~38.2% versus ~17.3%; $p < 0.01$; Figure 4C), suggesting that cotransplantation of NPCs and VPCs enhanced the vascular graft survival.

To compare the vascular differentiation capacity of grafted VPCs, we used LECTIN to label the vessels and quantified the number of Ho^+ nuclei within the LECTIN-perfused vessels out of the grafted Ho^+ nuclei (Figure 4D).

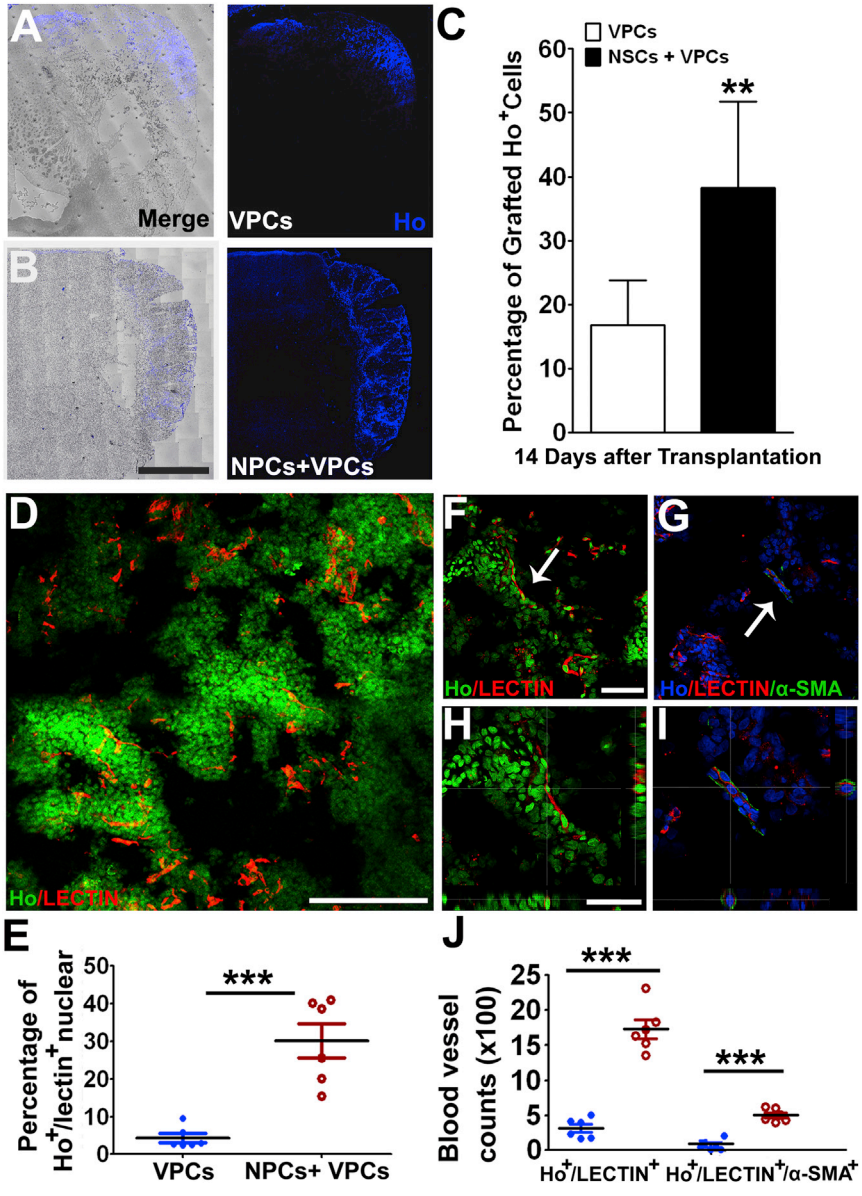

Figure 4. Cotransplantation of NPCs and VPCs Promoted Vascular Graft Survival and the Differentiation, Formation, and Maturation of Microvessels

(A and B) Low-magnification image of transplanted Ho^+ cells in rat brains in the group transplanted with VPCs alone (A) or the group cotransplanted with NPCs and VPCs (B) on day 14 after transplantation. Merge: merge of bright-field images with fluorescence images.

(C) The number of grafted Ho^+ cells out of the total number of injected Ho^+ cells in the group cotransplanted with NPCs and VPCs was compared with that in the group transplanted with VPCs alone on day 14 after transplantation.

(D) Representative image of LECTIN-perfused vessels derived from the Ho^+ VPCs.

(E) The number of Ho^+ nuclei within the LECTIN-perfused vessels relative to the number of grafted Ho^+ nuclei in the group cotransplanted with NPCs and VPCs was compared with that in the group transplanted with VPCs alone on day 14 after transplantation.

(F and G) High-magnification images of the Ho^+/LECTIN$^+$ or Ho^+/LECTIN$^+$/α-SMA$^+$ microvessels in (D).

(H and I) Magnified images of the arrow-marked microvessels in (F) and (G). The x-z and y-z planes of three-dimensional views are shown on the right and below, respectively.

(J) The numbers of Ho^+/LECTIN$^+$ or Ho^+/LECTIN$^+$/α-SMA$^+$ microvessels in the infarct area in the group cotransplanted with NPCs and VPCs were compared with those in the group transplanted with VPCs alone on day 14 after transplantation.

The data are presented as means ± SD (**$p < 0.01$, ***$p < 0.001$; Kruskal-Wallis test and Dunnett's post hoc). Scale bars, 2 mm in (B), 200 μm in (D), and 50 μm otherwise.

The proportion of Ho^+/LECTIN$^+$ nuclei in the rats cotransplanted with NPCs and VPCs was ~7.5-fold (~30.7% versus ~4.1%; $p < 0.001$) greater than in the rats transplanted with VPCs alone (Figure 4E), suggesting a significant improvement in the vascular differentiation capacity of grafted VPCs.

To determine whether cotransplantation of NPCs and VPCs can promote the formation of functional vessels derived from grafted VPCs, we counted the Ho^+/LECTIN$^+$ microvessels (Figures 4F and 4G) or mural cell-covered Ho^+/LECTIN$^+$ microvessels (Figures 4H and 4I) in the infarct area in both groups. We found ~5.4-fold more Ho^+/LECTIN$^+$ microvessels in the infarct area of rats cotransplanted with NPCs and VPCs compared with those transplanted with VPCs alone (17,287.0 ± 3,286.0 versus 3,198.0 ± 1,410.0, respectively; $p < 0.001$; Figure 4J). Similarly, immunostaining against α-SMA revealed that the number of Ho^+/LECTIN$^+$/α-SMA$^+$ microvessels in the infarct area of rats cotransplanted with NPCs and VPCs was ~10.8-fold greater (5,031.0 ± 909.6 versus 466.0 ± 355.0; $p < 0.001$; Figure 4J) than in rats transplanted with VPCs alone. It should be noted that we did not detect LECTIN$^+$ microvessels derived from the host in the infarct area in any of the groups examined.

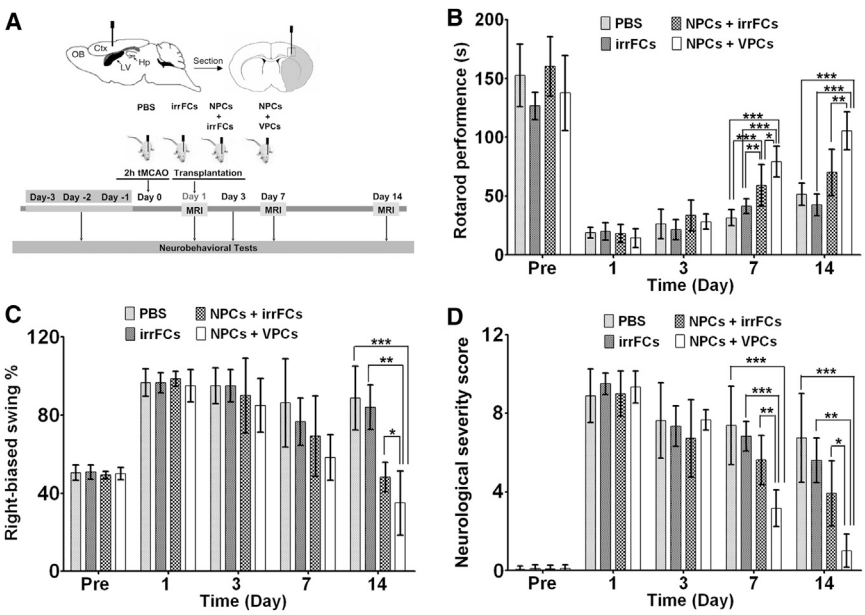

Figure 5. Cotransplantation of NPCs and VPCs More Effectively Improved the Neurobehavioral Deficits

(A) Diagram illustrating the experimental procedures used to evaluate neural behavioral performance and infarct volume changes in rats after various treatments. Sites of injection shown in sagittal planes and coronal planes are depicted on the left and right. OB, olfactory bulb; Ctx, cortex; LV, lateral ventricle; Hp, hippocampus. The infarct area is denoted in gray.

(B–D) The average rotarod performance (B), right-biased swing % (C), and mNSS (D) of rats in the group cotransplanted with NPCs and VPCs were compared with those in the group cotransplanted with NPCs and irrFCs, the group transplanted with irrFCs alone, and the group sham injected with PBS prior to cell transplantation (pre) and on days 3, 7, and 14 after cell transplantation (n = 18 for each group). The data are presented as means ± SD ($*p < 0.05$; $**p < 0.01$; $***p < 0.001$; B, one-way ANOVA and Tukey's post hoc; C and D, Kruskal-Wallis test and Dunnett's post hoc).

Cotransplantation of NPCs and VPCs More Effectively Improves Functional Neurological Deficits

To determine whether cotransplantation of NPCs and VPCs can promote functional recovery more effectively than transplantation of NPCs alone, we examined neurobehavioral parameters using the accelerating rotarod test, elevated body swing test (EBST), and modified neurological severity score (mNSS) test. For these tests, rats (n = 18) cotransplanted with 1 million NPCs and 0.5 million VPCs (25 μl/mice) were compared with rats (n = 18) transplanted with 1 million NPCs and 0.5 million irrFCs (25 μl/mice), rats (n = 18) transplanted with 1.5 million irrFCs alone (25 μl/mice), or rats (n = 18) sham injected with PBS (25 μl/mice; Figure 5A). The accelerating rotarod test provides an index of forelimb and hindlimb motor coordination and balance (Hamm et al., 1994). The rats displayed a significantly shorter duration of remaining on the accelerating rotarod on day 1 after stroke compared with before the stroke (17.4 ± 7.4 s versus 145.6 ± 29.0 s; $p < 0.001$; Figure 5B). On day 7, although the duration of remaining on the rotarod was significantly longer in rats cotransplanted with NPCs and irrFCs (59.1 ± 17.6 s) than in rats transplanted with irrFCs alone (35.2 ± 6.6 s; $p < 0.01$) or rats sham injected with PBS (31.6 ± 6.9 s; $p < 0.001$; Figure 5B), cotransplantation of NPCs and VPCs prolonged the duration of remaining on the rotarod more effectively than cotransplantation of NPCs and irrFCs at this time point (79.2 ± 13.2 s; $p < 0.05$; Figure 5B). On day 14, the rats cotransplanted with NPCs and VPCs still exhibited a significantly longer duration of remaining on the rotarod (105.5 ± 16.2 s) compared with rats cotransplanted with NPCs and irrFCs (70.2 ± 19.7 s; $p < 0.01$), transplanted with irrFCs alone (45.2 ± 7.4 s; $p < 0.001$), or sham injected with PBS (51.6 ± 9.4 s; $p < 0.001$; Figure 5B). In contrast, no difference was observed among the other three groups at this time point (Figure 5B).

In addition to the rotarod test, we performed the EBST to evaluate asymmetrical motor behavior (Borlongan and Sanberg, 1995). The rats exhibited a 100% tendency to turn toward the right side (contralateral to the lesion) on day 1 after stroke (Figure 5C). No difference was detected among the groups during the first 7 days (Figure 5C). On day 14, the percentage of right-biased swinging in rats cotransplanted with NPCs and VPCs (35.0% ± 15.7%) was significantly lower than that in rats cotransplanted with NPCs and irrFCs (69.2% ± 20.6%; $p < 0.01$), transplanted with irrFCs alone (84.0% ± 11.4%; $p < 0.001$), or sham injected with PBS (88.8% ± 16.4%; $p < 0.001$; Figure 5C). In contrast, no difference was observed among the other three groups at this time point (Figure 5C).

Finally, we used the mNSS test (14 points) to evaluate the motor abilities, reflexes, and balance of the rats (Boltze et al., 2006). On day 1 after stroke, all of the rats displayed a high mNSS (9.2 ± 1.0). On day 7, the rats cotransplanted with NPCs and VPCs displayed a significantly lower mNSS (3.2 ± 1.0) than the rats cotransplanted with NPCs and irrFCs (5.6 ± 1.3; $p < 0.01$), transplanted with irrFCs alone (6.8 ± 0.8; $p < 0.001$), or sham injected with PBS

(7.4 ± 2.0; $p < 0.001$; Figure 5D). By day 14, cotransplantation of NPCs and VPCs further reduced the mNSS. The mNSS of rats cotransplanted with NPCs and VPCs (1.0 ± 0.9) was significantly lower than that of rats cotransplanted with NPCs and irrFCs (3.9 ± 1.7; $p < 0.05$), transplanted with irrFCs alone (5.6 ± 1.1; $p < 0.01$), or sham injected with PBS (6.8 ± 2.3; $p < 0.001$; Figure 5D). In contrast, no difference was observed among the other three groups throughout the 14-day period (Figure 5D).

Cotransplantation of NPCs and VPCs More Effectively Attenuates the Infarct Volume

It was previously reported that T2-weighted MRI hyperintensity reflects vasogenic edema and cortical infarction, which constitute the total infarct volume during subacute stages from 24 hr to 2 weeks after stroke (Schiemanck et al., 2005). To assess whether cotransplantation of NPCs and VPCs could be more effective for attenuating infarct volume than transplantation of NPCs alone from day 1 to day 14 after stroke, we used T2-weighted MRI to detect the infarct volume in groups in which we had examined neurobehavioral parameters. Based on the T2 hyperintensity, the infarct volume was between 44% and 45% of the contralateral brain for all of the rats on day 1 after stroke (Figure 6A). After transplantation, the infarct volume (percentage of the contralateral hemisphere) of the rats cotransplanted with NPCs and VPCs (31.5% ± 2.5%) was significantly smaller than that of rats either transplanted with irrFCs alone (41.8% ± 5.9%; $p < 0.05$) or sham injected with PBS (40.9% ± 5.2%; $p < 0.01$) on day 7 (Figure 6B). No difference was detected between the rats cotransplanted with NPCs and VPCs and the rats cotransplanted with NPCs and irrFCs at this time point (Figure 6B). By day 14, the infarct volume of the rats cotransplanted with NPCs and VPCs (23.7% ± 1.2%) was significantly smaller than that of rats cotransplanted with NPCs and irrFCs (32.5% ± 5.2%; $p < 0.05$), transplanted with irrFCs alone (35.1% ± 5.4%; $p < 0.05$), or sham injected with PBS (36.9% ± 3.8%; $p < 0.001$; Figure 6B). In contrast, no difference was observed among the other three groups at this time point (Figure 6B).

Cotransplantation of NPCs and VPCs Promotes Engrafted Neural Cells Expressing VEGF, BDNF, and IGF1

To determine the molecular basis underlying the beneficial effect of cotransplantation of NPCs and VPCs, we examined the expression of a set of growth/trophic factors, including brain-derived neurotrophic factor (BDNF), vascular endothelial growth factor (VEGF), insulin growth factor 1 (IGF1), and nerve growth factor (NGF), by double immunostaining against cell-type-specific markers and growth/trophic proteins in all of the experimental groups. The immunostaining revealed that BDNF was expressed by a subset of the grafted $GFP^+/NESTIN^+$ NPCs (Figure 7A). BDNF was also synthesized by some $GFP^+/GFAP^+$ astroglia (Figure 7B). Aside from BDNF, many $GFP^+/GFAP^+$ cells expressed VEGF (Figure 7C). Notably, a subset of grafted $GFP^+/\beta III\text{-}TUBULIN^+$ neurons expressed IGF1 (Figure 7D). No detectable immunostaining against NGF was found in the infarct area. In addition, none of the Ho^+ vascular cells expressed any of the aforementioned growth/trophic factors in the rats cotransplanted with NPCs and VPCs or transplanted with VPCs alone. It should be noted that we did not detect growth/trophic factor-expressing cells derived from the host in the infarct area in any of the groups examined.

To assess whether cotransplantation of NPCs and VPCs could promote the neural production of growth/trophic factors, we counted the number of $GFP^+/NESTIN^+/BDNF^+$, $GFP^+/GFAP^+/BDNF^+$, $GFP^+/GFAP^+/VEGF^+$, and $GFP^+/\beta III\text{-}TUBULIN^+/IGF1^+$ cells in the infarct area in the group cotransplanted with NPCs and VPCs compared with either the group cotransplanted with NPCs and irrFCs or the group transplanted with NPCs alone on days 7 and 14. No difference in the numbers of growth/trophic factor expressing cells was observed between the control groups on either day 7 or 14 (Figure 7E). On day 7, the number of $GFP^+/NESTIN^+/BDNF^+$ cells in the group cotransplanted with NPCs and VPCs (696.6 ± 120.0) was ~2-fold greater than that in either the group transplanted with NPCs and irrFCs (325.0 ± 29.1; $p < 0.01$) or the group transplanted with NPCs alone (345.6 ± 40.11; $p < 0.05$; Figure 7E). No $GFP^+/NESTIN^+/BDNF^+$ cells were detected in any of the three groups on day 14, likely due to the full differentiation of $GFP^+/NESTIN^+$ cells (Figure 7E). Cotransplantation of NPCs and VPCs also promoted the production of BDNF in astroglia. The number of $GFP^+/GFAP^+/BDNF^+$ cells in the group cotransplanted with NPCs and VPCs (1,294.0 ± 136.2) was ~2.4-fold greater than that in the group cotransplanted with NPCs and irrFCs (5,31.3 ± 74.0; $p < 0.01$) or the group transplanted with NPCs alone (537.3 ± 65.9; $p < 0.01$) on day 7 (Figure 7E). By day 14, the group cotransplanted with NPCs and VPCs still displayed ~2-fold more $GFP^+/GFAP^+/BDNF^+$ cells (5,328.0 ± 201.3) than either the group cotransplanted with NPCs and irrFCs (2,606.0 ± 405.9; $p < 0.01$) or the group transplanted with NPCs alone (2,565.0 ± 1133.0; $p < 0.01$; Figure 7E). Similarly, the production of VEGF in astroglia was also enhanced after cotransplantation of NPCs and VPCs. The number of $GFP^+/GFAP^+/VEGF^+$ cells in the group cotransplanted with NPCs and VPCs (2,481.0 ± 366.6) was ~2.5-fold greater than that in the group cotransplanted with NPCs and irrFCs (995.7 ± 152.5; $p < 0.01$) and ~2.4-fold greater than that in the group transplanted with NPCs alone (1,026.0 ± 196.4; $p < 0.01$) on day 7. In contrast, no

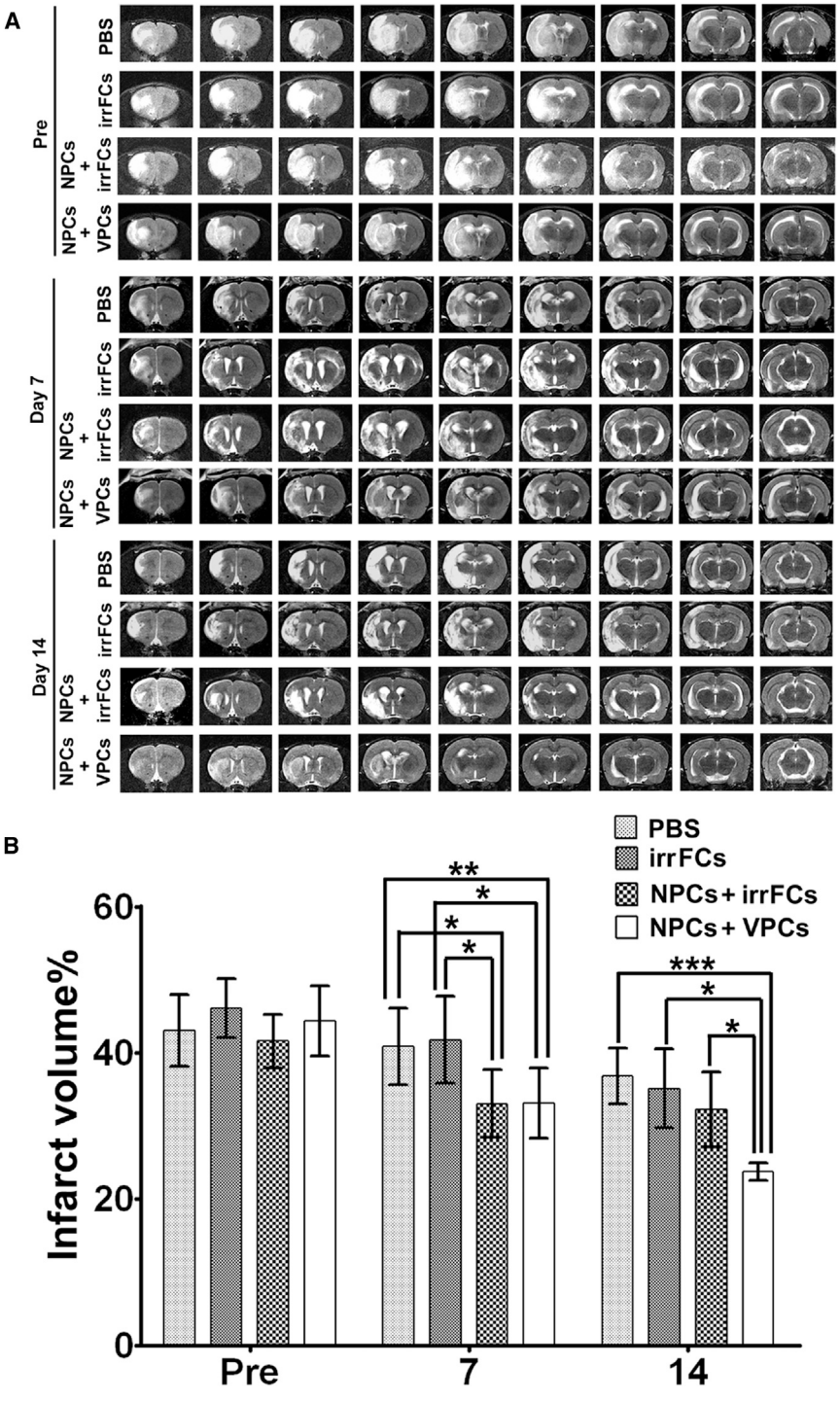

Figure 6. Cotransplantation of NPCs and VPCs More Effectively Attenuated the Cortical Infarct Volume

(A) Images captured via MRI of the same rats in each group prior to cell transplantation (pre) and on days 7 and 14 after cell transplantation.

(B) The average infarct volumes of rats evaluated by MRI in group cotransplanted with NPCs and VPCs were compared with those in the group cotransplanted with NPCs and irrFCs, the group transplanted with irrFCs alone, and the group sham injected with PBS on day 1 before cell transplantation and days 7 and 14 after cell transplantation (n = 18 for each group). The data are presented as means ± SD (*p<0.05; **p < 0.01; ***p < 0.001; Kruskal-Wallis test and Dunnett's post hoc).

difference was detected between the groups on day 14 (Figure 7E). Finally, the number of $GFP^+/\beta III\text{-}TUBULIN^+/IGF1^+$ cells in the group cotransplanted with NPCs and VPCs (1,460 ± 449.7) was ~5.3-fold greater than that in the group cotransplanted with NPCs and irrFCs (274.3 ± 17.6; $p < 0.01$) and ~5.0-fold greater than that in the group transplanted with NPCs alone (292.5 ± 34.5; $p < 0.01$) on day 7 (Figure 7E). By day 14, the number of $GFP^+/\beta III\text{-}TUBULIN^+/IGF1^+$ cells in the group cotransplanted with NPCs and VPCs (2,277.0 ± 262.4) was ~6.8-fold greater than that in the group cotransplanted with NPCs and irrFCs (335.9 ± 116.1; $p < 0.001$) and ~5.0-fold greater

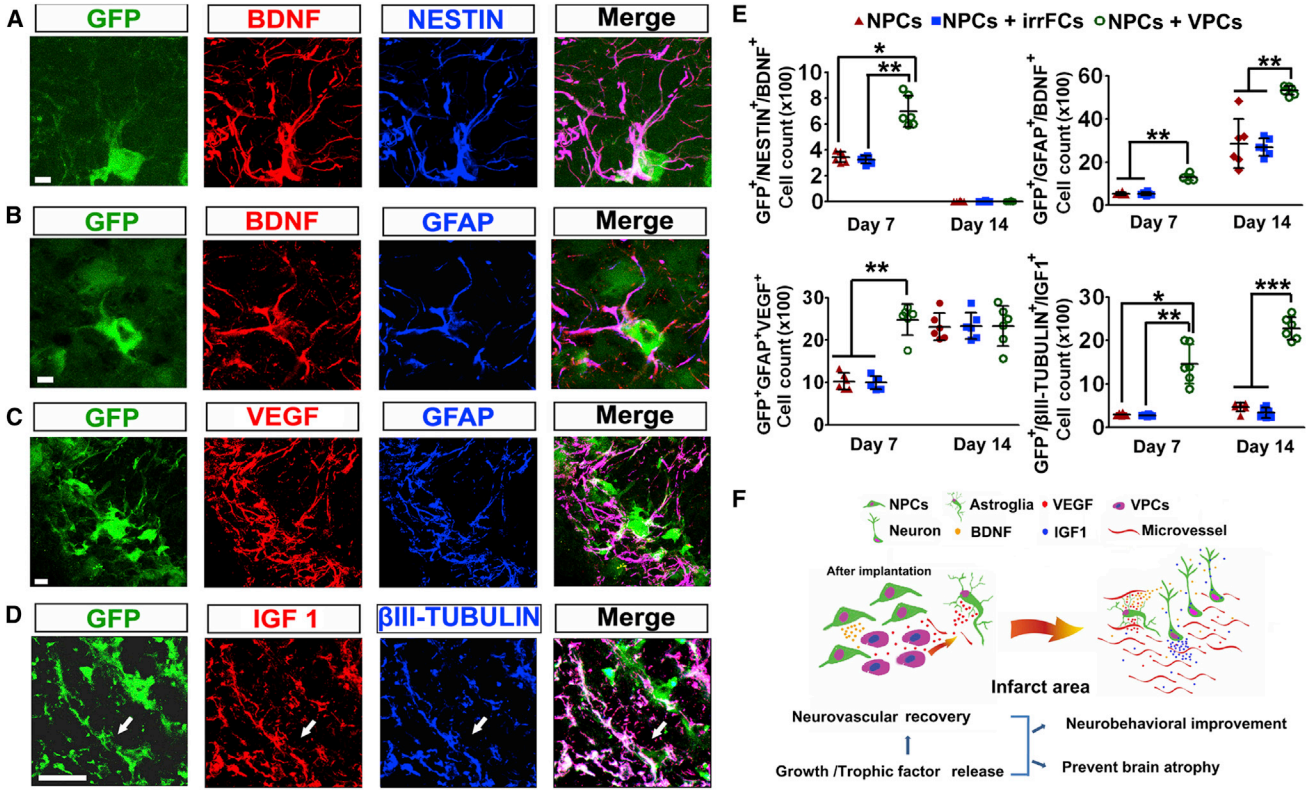

Figure 7. Cotransplantation of NPCs and VPCs Enhanced the Differentiation of VEGF-, BDNF-, and IGF1-Producing Neural Cells Derived from Transplanted NPCs

(A–D) Representative images of GFP$^+$/NESTIN$^+$/BDNF$^+$, GFP$^+$/GFAP$^+$/BDNF$^+$, GFP$^+$/GFAP$^+$/VEGF$^+$, and GFP$^+$/βIII-TUBULIN$^+$/IGF1$^+$ cells (arrow).

(E) The average total numbers of GFP$^+$/NESTIN$^+$/BDNF$^+$, GFP$^+$/GFAP$^+$/BDNF$^+$, GFP$^+$/GFAP$^+$/VEGF$^+$, and GFP$^+$/βIII-TUBULIN$^+$/IGF1$^+$ cells in the group cotransplanted with NPCs and VPCs were compared with those in the group cotransplanted with NPCs and irrFCs or the group transplanted with NPCs alone (n = 6 for each group) on day 7 or 14 after transplantation.

(F) Proposed model by which cotransplantation of NPCs and VPCs promotes neurovascular regeneration, infarct volume reduction, and recovery from functional neurological deficits. The data are presented as means ± SD (*p < 0.05; **p < 0.01; ***p < 0.001; Kruskal-Wallis test and Dunnett's post hoc). Scale bars, 20 μm.

than that in the group transplanted with NPCs alone (463.1 ± 106.7; p < 0.001; Figure 7E).

DISCUSSION

Numerous previous studies have described the transplantation of NPCs alone or ECs alone for the treatment of ischemic stroke (Liu et al., 2014). A recent study also demonstrated an enhanced functional recovery after cotransplantation of neural stem/progenitor cells and ECs (Nakagomi et al., 2009). However, in the present study, we cotransplanted ESC-VPCs with NPCs to treat ischemic stroke, which produced not only neural cells but also ECs and pericytes/SMAs, thus providing nearly all important components for recovery of the neurovascular unit. These beneficial outcomes appear to be due to the mutual support provided by each progenitor cell type and the enhanced expression of growth/trophic factors by grafted neural cells, which allow the cotransplanted progenitor cells to generate both the neural and vascular cell types that constitute the cerebral parenchyma (Figure 7F).

Rehabilitation after brain ischemia requires the recovery of both neural and vascular components in the damaged brain area. In this study, the cotransplanted NPCs and VPCs differentiated into neurons, astroglia, ECs, and mural cells in the infarct area. The latter two developed into microvessels or mural cell-covered microvessels. It was previously reported that endogenous neovascularization is poor in the infarct area after stroke in rats (Navaratna et al., 2009); however, we showed that the regeneration of microvessels derived from the transplanted VPCs was effective. These microvessels promoted the survival, differentiation, and maturation of neuronal cells derived from

the transplanted NPCs. Specifically, ~70% of the grafted NPCs generated neurons (βIII-TUBULIN$^+$). Approximately 17% of these neurons were mature neurons (TAU1$^+$) and ~32% were GABAergic neurons that displayed the ability to receive glutamatergic synaptic inputs, which may underlie the more effective improvement in motor coordination and balance of the rats based on the results of the rotarod, EBST, and mNSS tests during the 14 days after cotransplantation of NPCs and VPCs. Due to the lack of vascular supply, implanted NPCs display poor survival and differentiation into neuronal cells, ultimately risking graft failure in the group transplanted with NPCs alone or the group cotransplanted with NPCs and irrFCs. Supporting data for graft failure were generated in a preliminary long-term study of transplanted GFP$^+$ NPCs in the ischemic rat brain, in which no GFP$^+$ cells were detected on day 28 after stroke, whereas successfully engrafted and properly differentiated GFP$^+$ neural cells were detected upon cotransplantation of NPCs and VPCs at the same time point (data not shown). Consistent with these results, cotransplantation of NPCs and irrFCs did not improve some of the neurological parameters on day 7 and completely failed to display efficacy in neurobehavioral improvement on day 14. Reestablishing the vascular network in the infarct area appears to have a neuroprotective effect on neural transplants, and thus its importance for successful NPC transplantation therapy cannot be underestimated.

Stroke causes damage to not only a core area of the brain but also the peri-infarct area surrounding the ischemic core after the initial ischemic insult, which leads to enlargement of the infarct volume and, ultimately, irreversible tissue loss (Jung et al., 2013). This study demonstrates that cotransplantation of NPCs and VPCs prevents the progression of brain atrophy more effectively than cotransplantation of NPCs and irrFCs (~27% greater reduction in infarct volume). Post hoc immunohistochemical analysis revealed that cotransplantation of NPCs and VPCs induced the generation of more neurotrophic or angiogenic factor-producing neural cells than transplantation of NPCs, suggesting that cotransplantation of NPCs and VPCs has the potential to mediate a greater neuroprotective effect when these factors are delivered to both the infarct and peri-infarct cortex. In addition, the formation of mature microvessels in the infarct area by cotransplanted progenitor cells could exert a beneficial effect by increasing the blood flow, facilitating growth/trophic factor delivery. Thus, cotransplantation of NPCs and VPCs may provide mutually supportive trophic mechanisms of neural protection via production of VEGF, BDNF, and IGF1 in the microenvironment that preserve the host brain from further degeneration.

The expression of neurotrophic or angiogenic proteins by grafted neural cells benefits the two types of transplanted progenitors in the infarct core. First, BDNF, which is known to be neuroprotective (Louhivuori et al., 2011), may ensure the survival of newly formed neurons during the first week after transplantation. Second, VEGF, one of the most important angiogenic factors (Horie et al., 2011), and IGF1, considered as both neurotrophic and angiogenic (Zhu et al., 2009), may improve the neovascularization of transplanted VPCs throughout the 14 days after transplantation. Third, during the second week after transplantation, the strong expression of BDNF by newly engrafted astroglial cells may not only mediate consistent neuroprotection but also play a role in the control of the excitatory/inhibitory balance by regulating local GABAergic circuits (Jiao et al., 2011). The latter is important for proper neural network formation between the grafted and host neurons.

There are some limitations in the present study. First, we used Ho dye for in vivo tracking of grafted ESC-VPCs because these cells only undergo a relatively limited round of cell divisions before terminal differentiation occurs (Yamashita et al., 2000). The use of Ho dye to trace progenitor cells is similar to what was described in a previous study (Goodell et al., 1996). It should be pointed out that Ho dye is not an optimal tracer for lineage tracing because it becomes diluted along with cell divisions, which may result in an underestimation of the number of labeled cells at the endpoint. In addition, the debris of the dying Ho dye-labeled cells can be taken up by microphages, leading to false-positive results. Moreover, although the concentration of Ho dye we used for cell labeling does not cause apparent cell death (<0.01%), as evaluated by cytotoxicity tests for 3 consecutive days after the initial plating, higher concentrations of the dye can be toxic to cells and should be used with caution. Second, the majority of grafted fetal NPCs developed into GABAergic neuronal subtypes, and no glutamatergic neurons were generated. The lack of replacement for glutamatergic neurons might decrease glutamate production and consequently the glutamate pool in the infarct area, which would probably limit the extent of the restoration. Third, consistent with previous work by Nakagomi et al. (2009), this study reinforces the notion that cotransplantation of NPCs and ESC-VPCs for neurovascular regeneration is a better therapeutic strategy for the treatment of ischemic stroke than transplantation of NPCs alone. However, for therapeutic applications, it is desirable to derive NPCs and VPCs from the same donor, e.g., to derive these progenitors from the same pluripotent stem cells. Further studies could address whether using ESC-derived NPCs for cotransplantation would provide the same benefits as fetal NPCs.

EXPERIMENTAL PROCEDURES

Cell Culture

NPCs were isolated from the telencephalon of E14 GFP transgenic mice (Research Center of Nanjing University, Nanjing, China) as

described previously (Azari et al., 2011) and in Supplemental Experimental Procedures. To derive the VPCs, murine R1 ESCs (Institute of Biochemistry and Cell Biology, Shanghai, China) were cultured on mitomycin-C-treated feeder cells in ESC growth medium. Details regarding the methods used for ESC maintenance and differentiation can be found in Supplemental Experimental Procedures. The FLK1$^+$ cell fraction from day 4 EBs was isolated using a flow cytometer (Beckman-Coulter). The FLK1$^+$ cells were either immediately used for cell transplantation or seeded on fibroblasts treated with mitomycin-C (Sigma), and exposed to 50 ng/ml VEGF (R&D Systems) for in vitro experiments.

tMCAO

To induce focal cerebral ischemia, adult male rats (Sprague-Dawley, 3 months old, 250–300 g; Shanghai Laboratory Animal Center, Shanghai, China) were subjected to tMCAO for 2 hr. MRI was performed 24 hr after tMCAO. Only rats that displayed an infarct volume between 41% and 44% of the contralateral hemisphere were used for all of the experiments in the study. Animal surgeries were performed as previously described (Yang and Betz 1994) and in Supplemental Experimental Procedures. All animal procedures were approved by the Shanghai Jiaotong University Administrative Panel on Laboratory Animal Care.

Cell Transplantation

Cells were transplanted into the peri-infarct area at 24 hr after ischemic stroke in rats. To track VPCs and irrFCs after transplantation, the VPCs or irrFCs were incubated in Hoechst 33342 (Sigma-Aldrich) medium (7.5 μg/ml) for 5 min at 37°C. The rats were treated with 25 μl of the cell suspension at the densities indicated in Results or with PBS along the anterior-posterior axis in the cortex at the coordinates described in Supplemental Experimental Procedures. The rats were injected i.p. daily with cyclosporine A (CsA, 10 mg/kg; Sigma-Aldrich) for immunosuppression from day 1 to day 14 after cell transplantation. On day 7 or day 14, the rats were transcardially perfused with heparinized saline (0.9%) and fixed with 4% paraformaldehyde (PFA). Five equidistant sets of coronal sections (20 μm thick) were generated using a cryostat and stored in cryoprotectant solution at −80°C until use.

Cell Migration

Fourteen days after transplantation, transplants were visualized by fluorescence microscopy. The migration of transplanted cells in rat brain slices was quantified in terms of the maximum distance. For each transplant, cells that had migrated the farthest from the edge of the transplants were measured. In each rat, the average from three coronal slices was obtained. The average of vertical distance of the farthest migration from multiple transplants is presented in Figure 2E. Six brains were analyzed for each group.

MRI

All MRI experiments were performed using a 3T General Electric MR system (GE Medical Systems). The brains were examined via T2-weighted MRI using the imaging parameters described in Supplemental Experimental Procedures. Subsequent measurement processing was performed using ImageJ and MRI Cell Image Analyzer (Montpellier RIO Imaging Volker Baecker) software. The infarct volume was calculated based on the following formula: (volume in the contralateral hemisphere − noninfarct volume in the ipsilateral hemisphere) / volume in the contralateral hemisphere × 100%.

In Vivo LECTIN-DyLight 594 Angiography

LECTIN-DyLight 594 (Vector Laboratories) was administered to anesthetized rats via the femoral vein 5 min before they were sacrificed on day 14. The rats were then transcardially perfused with ice-cold heparinized PBS and their brains were isolated and embedded in Tissue-Tek O.C.T. compound (Sakura Finetek).

Neurobehavioral Tests

All neurobehavioral tests were performed by an investigator who was blinded to the experimental groups. The rats were trained for 3 consecutive days prior to surgery. Neurobehavioral tests were performed before stroke occurred and on days 1, 3, 7, and 14 after the stroke. Details regarding the methods used for the rotarod, EBST, and mNSS tests can be found in Supplemental Experimental Procedures.

Immunofluorescence Staining

Brain sections were fixed and stained with the appropriate antibodies. Details regarding the immunostaining procedures and primary antibodies used for immunofluorescence can be found in Supplemental Experimental Procedures. The primary antibodies were detected using the appropriate secondary antibodies conjugated to Alexa Fluor 488, 594, or 633 (Jackson ImmunoResearch). Images were viewed under a laser-scanning confocal microscope (TCS SP5II; STED CW; Leica). Serial images were captured along the z axis every 1 μm to a depth of 20 μm.

Cell Counting

Brains were sectioned at 20 μm intervals from approximately +1 mm and −5 mm to bregma. Every ninth section of the serial sections was collected, placed on the slide, and processed/counted for GFP$^+$ cells, Ho$^+$ cells, or LECTIN-perfused vessels, or stained with antibodies against the cell-type-specific markers or growth/trophic proteins. Images were captured using a laser-scanning confocal microscope. To estimate the total cell number in a whole brain, we counted the total numbers of cells or positively stained cells in one set of serial sections (containing every ninth section) and then multiplied them by nine.

RNA Extraction and RT-PCR

Total RNA was isolated from undifferentiated ESCs and FLK1$^+$ and FLK1$^-$ cell fractions from day 4 EBs using Trizol (Invitrogen). The RNA was treated with DNase I (Invitrogen) to eliminate any contaminating DNA. RT-PCRs were performed using SuperScript III (Invitrogen) according to the manufacturer's instructions. The primer sequences used for this study can be found in Supplemental Experimental Procedures.

Statistical Analysis

The results are presented as the means ± SD and were analyzed via the unpaired t test, the Kruskal-Wallis test, or one-way ANOVA.

Post hoc comparisons were conducted using either Tukey's or Dunnett's test. Statistical analysis was performed using PRISM software (GraphPad).

SUPPLEMENTAL INFORMATION

Supplemental Information includes Supplemental Experimental Procedures and one figure and can be found with this article online at http://dx.doi.org/10.1016/j.stemcr.2014.05.012.

AUTHOR CONTRIBUTIONS

J.L. designed and conducted the experiments and wrote the manuscript. Y.H.T. coconducted the experiments and participated in data collection. Y.T.W., R.B.T., and W.F.J. contributed to the experiments. W.-Q.G. and G.-Y.Y. did the conceptual designs, interpreted the results, and edited and approved the final version of the manuscript.

ACKNOWLEDGMENTS

This work was supported by the Chinese Ministry of Science and Technology (2012CB966800, 2013CB945600, and 2012CB967903 to W.-Q.G., and 2011CB504405 to G.-Y.Y. and Y.T.W.), the National Natural Science Foundation of China (81130038 and 81372189 to W.-Q.G., 81302235 to J.L., and 81070939 to G.-Y.Y.), the Key Discipline and Specialty Foundation of Shanghai Health Bureau (to W.-Q.G.), the Science and Technology Commission of Shanghai Municipality (Pujiang Program to W.-Q.G. and 10JC1408100 to G.-Y.Y.), the Shanghai Education Committee Key Discipline and Specialty Foundation (J50208 to W.-Q.G.), the K.C. Wong Foundation (to W.-Q.G. and G.-Y.Y.), and the China Postdoctoral Science Foundation (20110490737 to J.L.).

Received: December 31, 2013
Revised: May 15, 2014
Accepted: May 15, 2014
Published: June 19, 2014

REFERENCES

Azari, H., Sharififar, S., Rahman, M., Ansari, S., and Reynolds, B.A. (2011). Establishing embryonic mouse neural stem cell culture using the neurosphere assay. J. Vis. Exp. *47*, e2457.

Boltze, J., Kowalski, I., Förschler, A., Schmidt, U., Wagner, D., Lobsien, D., Emmrich, J., Egger, D., Kamprad, M., Blunk, J., and Emmrich, F. (2006). The stairway: a novel behavioral test detecting sensomotoric stroke deficits in rats. Artif. Organs *30*, 756–763.

Borlongan, C.V., and Sanberg, P.R. (1995). Elevated body swing test: a new behavioral parameter for rats with 6-hydroxydopamine-induced hemiparkinsonism. J. Neurosci. *15*, 5372–5378.

Dalkara, T., Gursoy-Ozdemir, Y., and Yemisci, M. (2011). Brain microvascular pericytes in health and disease. Acta Neuropathol. *122*, 1–9.

Goodell, M.A., Brose, K., Paradis, G., Conner, A.S., and Mulligan, R.C. (1996). Isolation and functional properties of murine hematopoietic stem cells that are replicating in vivo. J. Exp. Med. *183*, 1797–1806.

Hamm, R.J., Pike, B.R., O'Dell, D.M., Lyeth, B.G., and Jenkins, L.W. (1994). The rotarod test: an evaluation of its effectiveness in assessing motor deficits following traumatic brain injury. J. Neurotrauma *11*, 187–196.

Horie, N., Pereira, M.P., Niizuma, K., Sun, G., Keren-Gill, H., Encarnacion, A., Shamloo, M., Hamilton, S.A., Jiang, K., Huhn, S., et al. (2011). Transplanted stem cell-secreted vascular endothelial growth factor effects poststroke recovery, inflammation, and vascular repair. Stem Cells *29*, 274–285.

Jiao, Y., Zhang, Z., Zhang, C., Wang, X., Sakata, K., Lu, B., and Sun, Q.Q. (2011). A key mechanism underlying sensory experience-dependent maturation of neocortical GABAergic circuits in vivo. Proc. Natl. Acad. Sci. USA *108*, 12131–12136.

Jung, S., Gilgen, M., Slotboom, J., El-Koussy, M., Zubler, C., Kiefer, C., Luedi, R., Mono, M.L., Heldner, M.R., Weck, A., et al. (2013). Factors that determine penumbral tissue loss in acute ischaemic stroke. Brain *136*, 3554–3560.

Kaneko, Y., Tajiri, N., Shinozuka, K., Glover, L.E., Weinbren, N.L., Cortes, L., and Borlongan, C.V. (2012). Cell therapy for stroke: emphasis on optimizing safety and efficacy profile of endothelial progenitor cells. Curr. Pharm. Des. *18*, 3731–3734.

Li, J., and Stuhlmann, H. (2012). In vitro imaging of angiogenesis using embryonic stem cell-derived endothelial cells. Stem Cells Dev. *21*, 331–342.

Liu, X., Ye, R., Yan, T., Yu, S.P., Wei, L., Xu, G., Fan, X., Jiang, Y., Stetler, R.A., Liu, G., and Chen, J. (2014). Cell based therapies for ischemic stroke: from basic science to bedside. Prog. Neurobiol. *115*, 92–115.

Lopes, M., Goupille, O., Saint Cloment, C., Lallemand, Y., Cumano, A., and Robert, B. (2011). Msx genes define a population of mural cell precursors required for head blood vessel maturation. Development *138*, 3055–3066.

Louhivuori, V., Vicario, A., Uutela, M., Rantamäki, T., Louhivuori, L.M., Castrén, E., Tongiorgi, E., Akerman, K.E., and Castrén, M.L. (2011). BDNF and TrkB in neuronal differentiation of Fmr1-knockout mouse. Neurobiol. Dis. *41*, 469–480.

Lugus, J.J., Park, C., Ma, Y.D., and Choi, K. (2009). Both primitive and definitive blood cells are derived from Flk-1+ mesoderm. Blood *113*, 563–566.

Martino, G., and Pluchino, S. (2006). The therapeutic potential of neural stem cells. Nat. Rev. Neurosci. *7*, 395–406.

Moskowitz, M.A., Lo, E.H., and Iadecola, C. (2010). The science of stroke: mechanisms in search of treatments. Neuron *67*, 181–198.

Nakagomi, N., Nakagomi, T., Kubo, S., Nakano-Doi, A., Saino, O., Takata, M., Yoshikawa, H., Stern, D.M., Matsuyama, T., and Taguchi, A. (2009). Endothelial cells support survival, proliferation, and neuronal differentiation of transplanted adult ischemia-induced neural stem/progenitor cells after cerebral infarction. Stem Cells *27*, 2185–2195.

Navaratna, D., Guo, S., Arai, K., and Lo, E.H. (2009). Mechanisms and targets for angiogenic therapy after stroke. Cell Adhes. Migr. *3*, 216–223.

Reynolds, B.A., and Weiss, S. (1996). Clonal and population analyses demonstrate that an EGF-responsive mammalian embryonic CNS precursor is a stem cell. Dev. Biol. *175*, 1–13.

Schiemanck, S.K., Post, M.W., Witkamp, T.D., Kappelle, L.J., and Prevo, A.J. (2005). Relationship between ischemic lesion volume and functional status in the 2nd week after middle cerebral artery stroke. Neurorehabil. Neural Repair *19*, 133–138.

van der Worp, H.B., and van Gijn, J. (2007). Clinical practice. Acute ischemic stroke. N. Engl. J. Med. *357*, 572–579.

Yamashita, J., Itoh, H., Hirashima, M., Ogawa, M., Nishikawa, S., Yurugi, T., Naito, M., Nakao, K., and Nishikawa, S. (2000). Flk1-positive cells derived from embryonic stem cells serve as vascular progenitors. Nature *408*, 92–96.

Yang, G.Y., and Betz, A.L. (1994). Reperfusion-induced injury to the blood-brain barrier after middle cerebral artery occlusion in rats. Stroke *25*, 1658–1664, discussion 1664–1665.

Zhu, W., Fan, Y., Hao, Q., Shen, F., Hashimoto, T., Yang, G.Y., Gasmi, M., Bartus, R.T., Young, W.L., and Chen, Y. (2009). Postischemic IGF-1 gene transfer promotes neurovascular regeneration after experimental stroke. J. Cereb. Blood Flow Metab. *29*, 1528–1537.

Zlokovic, B.V. (2010). Neurodegeneration and the neurovascular unit. Nat. Med. *16*, 1370–1371.